Journal of Materials Chemistry A

PAPER

View Article Online
View Journal | View Issue



Cite this: J. Mater. Chem. A, 2014, 2, 20605

# Microwave-assisted solvothermal preparation of nitrogen and sulfur co-doped reduced graphene oxide and graphene quantum dots hybrids for highly efficient oxygen reduction†

Zhimin Luo,‡[a] Dongliang Yang,‡[a] Guangqin Qi,[a] Jingzhi Shang,[c] Huanping Yang,[d] Yanlong Wang,[c] Lihui Yuwen,[a] Ting Yu,*[c] Wei Huang*[ab] and Lianhui Wang*[a]

Received 25th September 2014
Accepted 27th October 2014

DOI: 10.1039/c4ta05096g

www.rsc.org/MaterialsA

A facile solvothermal method assisted by microwave irradiation was developed for preparing nitrogen and sulfur co-doped reduced graphene oxide functionalized with fluorescent graphene quantum dots (N,S-RGO/GQDs). Graphene quantum dots (GQDs) show high fluorescence and excitation-dependent fluorescent properties. The resultant N,S-RGO/GQDs hybrids as a kind of metal-free electrocatalyst were demonstrated to have good catalytic properties with long-term operational stability and tolerance to the crossover effects of methanol for oxygen reduction *via* a four-electron pathway in alkaline solution. This research not only develops a low-cost, economic and scalable approach for preparing a metal-free electrocatalyst for the oxygen reduction reaction (ORR), but also produces nitrogen and sulfur co-doped graphene quantum dots (N,S-GQDs) with high fluorescent characteristics.

## Introduction

The synthesis of efficient and low-cost catalysts for the oxygen reduction reaction (ORR) is very important in the development of fuel cells.[1–3] So far, the general catalysts used for ORR in the cathodes of commercial fuel cells are still platinum-based materials. However, their extensive application has been weakened by the high cost and poor durability of platinum.[4,5] Therefore, great efforts have been made to reduce or replace catalysts based on Pt. For example, developing non-precious-metal as well as metal-free catalysts for ORR is most active and competitive.[3,6,7]

Heteroatom-doped carbon nanomaterials have been researched as metal-free catalysts for ORR.[8] Previous reports have confirmed that the doping of heteroatoms (N, P, B) into graphene or carbon nanotubes can effectively modify their intrinsic properties including their electrochemical activities.[9,10] For instance, nitrogen-doped carbon nanotubes[1,11,12] and graphene[8,13–15] have shown good electrocatalytic properties and are considered to be promising for the replacement of commercial catalysts based on platinum, but are still on a less-competitive level.[3,10] It is believed that there are two limitations for their applications in fuel cells. On one hand, nitrogen-doping of carbon nanotubes or graphene inevitably needs to be carried out at high temperatures, which encumbers their large-scale production and application in fuel cells.[9,16] On the other hand, the low surface density of catalytic sites influences their catalytic activity.[13,17,18]

Microwave-assisted and solvothermal methods are known for their high efficiency, simple operation, mild synthesis conditions, and capability to deliver relatively large quantities.[13] Graphene quantum dots (GQDs) have special properties including their quantum confinement and higher surface-to-volume ratio.[19–24] GQDs prepared from graphene oxide (GO) are soluble in water and common organic solvents, which can self-assemble on the surface of reduced graphene oxide (RGO) to prevent aggregation in the procedure of reducing GO in the solution.[20] Furthermore, doping GQDs with heteroatoms has proved to have enhanced fluorescence and electrocatalytic activity for ORR.[19] Furthermore, the larger specific surface area

[a]Jiangsu Key Laboratory for Organic Electronics & Information Displays, Institute of Advanced Materials, Nanjing University of Posts and Telecommunications, Nanjing 210023, PR China. E-mail: iamlhwang@njupt.edu.cn

[b]Jiangsu-Singapore Joint Research Center for Organic/Bio-Electronics & Information Displays, Institute of Advanced Materials, Nanjing Tech University, Nanjing 211816, PR China. E-mail: iamwhuang@njupt.edu.cn

[c]Division of Physics and Applied Physics, School of Physical and Mathematical Sciences, Nanyang Technological University, 21 Nanyang Link, Singapore 637371. E-mail: yuting@ntu.edu.sg

[d]Department of Science, Zhejiang University of Science and Technology, Hangzhou, Zhejiang 310023, PR China

† Electronic supplementary information (ESI) available: XPS spectra and catalytic property of N,S-GQDs; LSV measurements of the commercial Pt/C catalyst; XPS spectra, CVs, and LSV results for N,S-RGO/GQDs hybrids annealed at 800 °C for 2 h in Ar; TEM and TEM images of N,S-RGO/GQDs after cycle durability tests; comparison of ORR catalytic performances between N,S-RGO/GQDs hybrids and other doped carbon materials in the literature. See DOI: 10.1039/c4ta05096g

‡ These authors contributed equally to this article.

of heteroatom-doped GQDs can result in their higher surface density of catalytic sites.

In this work, we developed a solvothermal approach assisted by microwave irradiation to synthesize nitrogen and sulfur co-doped GQDs (N,S-GQDs) and RGO/GQDs hybrids (N,S-RGO/GQDs). The solution chemistry process for the synthesis of N,S-GQDs or N,S-RGO/GQDs hybrids is based on the reaction of GO and reduced glutathione in *N*,*N*-dimethylformamide (DMF) at 200 °C under microwave irradiation. N,S-RGO/GQDs hybrids exhibit excellent electrocatalytic activity and show good potential prospects as low-cost, metal-free electrochemical catalysts for ORR to replace commercial Pt/C catalysts. N,S-GQDs, as a by-product, emit strong blue fluorescence at 350 nm excitation. In view of the simple and one-pot preparation process, this method is favorable for the synthesis of fluorescent N,S-GQDs, and N,S-RGO/GQDs hybrids as metal-free catalysts for ORR on a large scale.

## Experimental

### Synthesis of N,S-RGO/GQDs hybrids

Firstly, GO was prepared by the modified Hummers's method according to our previous reports.[41–43] 40 mg of GO was added into the mixed acid ($H_2SO_4$ : $HNO_3$ = 1 : 3) and ultrasonicated for 5 min. Then, the mixed suspension was refluxed for 12 h at 70 °C and subsequently added into 160 mL of deionized water. The GO and the mixed acid were separated through filtration with a microporous membrane (pore size 0.22 μm), and rinsed with deionized water. The as-prepared GO was dispersed in 50 mL DMF and ultrasonicated for 9 h. 20 mg of reduced glutathione was added into 20 mL of the colloidal solution. The mixed solution was transferred to a quartz tube and reacted at 200 °C for 12 h under microwave irradiation. The prepared solution was centrifuged at 8000 rpm for 15 min. The upper solution was N,S-GQDs in DMF and the deposition was purified with deionized water to get N,S-RGO/GQDs hybrids.

### Preparation of the modified electrode

A glassy carbon electrode (3 mm diameter) (GCE) was polished successively with 1.0, 0.3 and 0.05 μm α-alumina powders, and ultrasonicated in ethanol and deionized water for short time to clean it. Then, the electrode was rinsed with deionized water and dried at room temperature.[42] 7 mg of N,S-RGO/GQDs hybrids or the commercial Pt/C catalyst (10 wt% Pt on carbon black) was dispersed in the 1.40 mL deionized water and ultrasonicated for 30 min to form a suspension with a concentration of 5 mg $mL^{-1}$. The modified GCE were prepared by dropping 5 μL of the N,S-RGO/GQDs hybrids or Pt/C suspension (5 mg $mL^{-1}$) onto the surface of prepolished GCE and drying at room temperature. 5 μL 1% Nafion solution was dropped on the surface of the modified GCE and dried at room temperature to form the working electrodes for cyclic voltammogram (CV) measurements. Rotating disk electrode (RDE) coated with 5 μL N,S-RGO/GQDs hybrids or Pt/C suspension (5 mg $mL^{-1}$) was used for linear sweep voltammetry (LSV) measurements.

### Electrochemical measurements

All electrochemical measurements were performed at room temperature in 0.1 M KOH solutions, which were purged with nitrogen or oxygen for at least 30 min prior to each measurement. The modified electrodes were used as the working electrode with a Ag/AgCl (saturated by 3 M KCl) electrode as the reference and a platinum wire as the counter electrode. LSV measurements were performed with different rotary speeds from 100 to 2400 rpm.

### Characterizations

Transmission electron microscopy (TEM) and high-resolution transmission electron microscopy (HRTEM) images of N,S-RGO/GQDs hybrids and N,S-GQDs were recorded on a JEOL JEM-2011F electron microscope operated at 200 kV. X-Ray diffraction (XRD) patterns were obtained using a Philips Xpert X-ray diffractometer using Cu KR radiation at $\lambda = 1.5418$ Å. XPS characterization was performed on the XPS spectrometer (QUANTUM 2000, Physical Electronics, USA) by using focused monochromatized Al Kα radiation (1486.6 eV). The UV-vis absorption spectra were measured by using UV-vis-NIR spectrophotometer (Shimadzu, UV-3150). Raman characterization was carried out with a 633 nm micro-Raman spectrometer (Renishaw INVIA Reflex) with a 1800 lines per mm grating at room temperature.

## Results and discussion

N,S-RGO/GQDs hybrids and N,S-GQDs were synthesized through a one-step solvothermal process assisted by microwave irradiation (Scheme 1). GO of small size was firstly prepared by the modified Hummers's method[25] and dispersed in DMF. Then, reduced glutathione as a nitrogen and sulfur precursor was added to the GO/DMF dispersion. The mixture of GO and reduced glutathione was heated at 200 °C under microwave irradiation for 12 h. Some of the N,S-GQDs were patterned on N,S-RGO through covalent and non-covalent interaction. Most N,S-GQDs were dispersed in DMF. The N,S-RGO/GQDs hybrids were separated by centrifugation, and N,S-GQDs in the upper solution were prepared after DMF and excessive reduced glutathione were removed by rotary evaporation and dialysis.

The prepared N,S-RGO/GQDs hybrids were investigated by HRTEM. As shown in Fig. 1A and B, fairly uniform N,S-GQDs

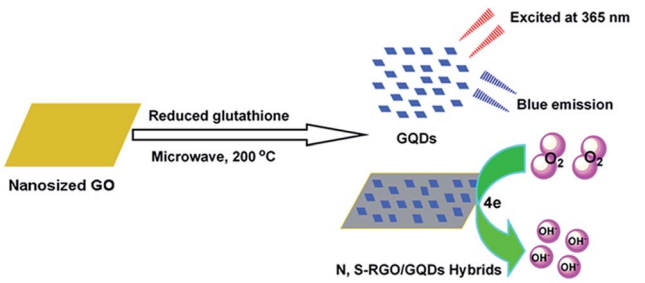


Scheme 1 Preparation of fluorescent GQDs, and N,S-RGO/GQDs hybrids for ORR.

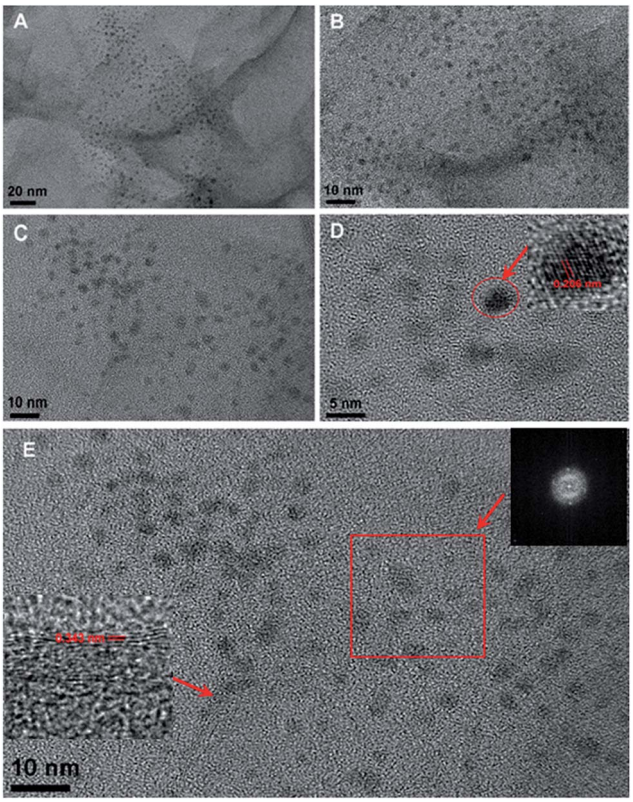


Fig. 1 Low-magnification (A) and high-magnification (B–E) TEM images of N,S-RGO/GQDs hybrids. Inset of (D) is the crystal plane of N,S-GQDs. Insets of (E) shows the corresponding Fourier transform of the corresponding HRTEM image in the red frame (upper corner), and the crystal plane of N,S-RGO sheets (lower corner), respectively.

with a diameter of 1.5–4.0 nm are dispersed on a sheet of RGO doped with nitrogen and sulfur (N,S-RGO), which are similar to GQDs or N-doped GQDs prepared by the electrochemical method.[19,23] HRTEM images (Fig. 1C and D) and Fourier transform spectra of the corresponding HRTEM image (inset of Fig. 1E) indicate that the interlayer distance of N,S-GQDs is 0.206 nm, which is the same as the interplanar distance of diamond ($d_{111}$ = 0.206 nm).[26,27] The inset (lower corner) in Fig. 1E illustrates a multilayered structure of graphene with a lattice spacing of 0.343 nm that is very close to the (002) lattice spacing of graphite ($d_{002}$ = 0.34 nm).[28]

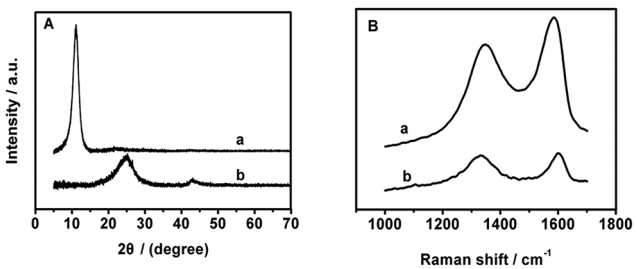


Fig. 2 XRD (A) and Raman spectra (B) of GO (a) and N,S-RGO/GQDs hybrids (b).

The crystal phases of GO and N,S-RGO/GQDs hybrids were determined by XRD. As shown in Fig. 2, the diffraction pattern of GO has a peak centered at $2\theta = 11.05°$, corresponding to the (001) reflection with interlayer spacing of 7.99 Å. After GO was reacted with reduced glutathione for 12 h at 200 °C under microwave irradiation, the XRD peak of GO disappeared, but two new broad diffraction peaks at $2\theta$ values of 25.0° and 43.0° in N,S-RGO/GQDs hybrids appeared, which are close to the typical (002) diffraction peak ($d$-spacing 3.35 Å at $2\theta = 26.6°$) of graphite and (111) diffraction peak ($d$-spacing 2.06 Å at $2\theta$ = 43.98°) of diamond.[27,28] These results confirmed that GO was reduced at 200 °C in the DMF under microwave irradiation. Raman spectra of GO and N,S-RGO/GQDs hybrids are included in Fig. 2B. It is observed that N,S-RGO/GQDs hybrids present Raman peaks centered at 1333 and 1604 $cm^{-1}$ resulting from the typical D and G band respectively, which are similar to the nitrogen-doped GQDs prepared by the electrochemical method.[19] This indicates that N,S-GQDs have been assembled on the N,S-RGO. N,S-RGO/GQDs hybrids have an $I_D/I_G$ ratio of 0.84, which is much lower than that of nitrogen-doped graphene or sulfur-doped graphene in other reports,[4,29] indicating the formation of larger crystalline graphitic domains in N,S-RGO/GQDs hybrids.

The surface composition and elemental analysis of the N,S-RGO/GQDs hybrids were characterized by X-ray photoelectron spectroscopy (XPS). As seen from the survey scan of N,S-RGO/GQDs hybrids in Fig. 3A, the N/C atomic ratio of N,S-RGO/GQDs hybrids was calculated to be 4.74%, which is comparable to that of N-doped graphene[8] and GQDs[19] reported previously. The S/C atomic ratio of N,S-RGO/GQDs hybrids is about 1.76%. The N1s spectrum (Fig. 3B) shows four peaks at 398.4, 399.3, 400.5 and 402.3 eV, which are attributed to the pyridinic-N, pyrrolic-N, and N-oxides of N,S-RGO/GQDs hybrids, respectively.[30] The S2p spectrum of N,S-RGO/GQDs hybrids is displayed in Fig. 3c. The five peaks in Fig. 3c are attributed to three different sulfur species. The first and the second doublet

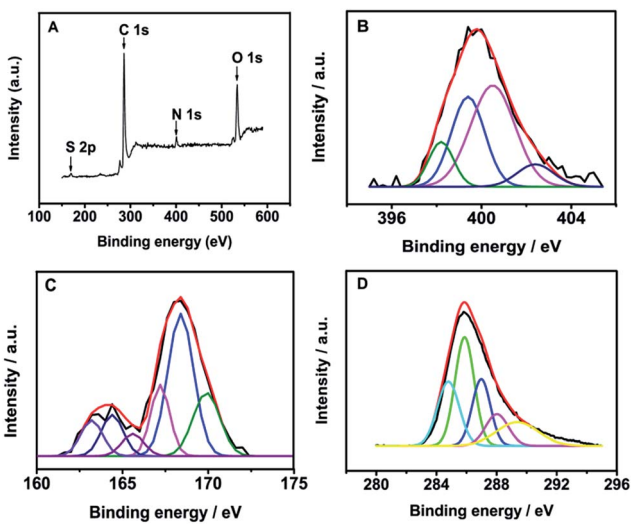


Fig. 3 XPS survey for N,S-RGO/GQDs hybrids (A) and high resolution N1s (B), S2p (C), C1s (D) XPS spectra of N,S-RGO/GQDs hybrids.

at 163.2, 164.5 and 165.6 eV originate from the core levels of sulfur in thiol, thiophene and benzothiadiazole, respectively.[31] The peaks at 167.2, 168.4 and 170.0 eV are assigned to the oxidized sulfur groups (–C–$SO_x$–C–, $x$ = 2–4, at 167.5–171.5 eV) such as sulfate or sulfonate.[10] Recent studies suggest that the enhanced electrocatalytic activity of nitrogen-doped graphene is due to the pyridinic-N, pyrrolic-N or graphitic-N (quaternary nitrogen).[30] Furthermore, the increased electrocatalytic activity of sulfur-doped graphene is related to the formation of thiophene or benzothiadiazole-like structures with neighboring carbon atoms, and the oxidized sulfur groups are chemically inactive for ORR.[10] XPS characterization indicates that the N,S-RGO/GQDs hybrids contain advantageous structures for ORR, including pyridinic-N, pyrrolic-N, thiophene or benzothiadiazole-like structures.

The doping of nitrogen and sulfur in N,S-GQDs was confirmed by the XPS characterization in Fig. S1.† The optical properties of dissociative N,S-GQDs were investigated by UV-vis absorption and fluorescent measurements. From the UV-vis absorption spectrum of the N,S-GQDs (Fig. 4A), a typical absorption peak at about 337 nm was observed, which is similar to that of the reported GQDs.[32,33] The fluorescent emission spectra show a strong peak at 425 nm as well as a shoulder peak at 442 nm when excited at 320 nm (Fig. 4C), and only a strong peak at 425 nm at the excitation of 350 nm. The full width at half maximum (FWHM) is about 89 nm, which is smaller than that of reported GQDs.[24,32–34] The inset in Fig. 4B is a photograph of the N,S-GQDs aqueous solution with bright blue fluorescence under UV light ($\lambda$ = 365 nm). Using quinine sulfate as a reference, the fluorescent quantum yield was measured to be 11.7%, which is higher than those of reported fluorescent carbon nanomaterials.[24,32,33] It is found that the fluorescent spectra of N,S-GQDs are dependent on the excitation wavelengths. The main fluorescent emission peak shifts to the longer wavelength when the excitation wavelength is changed from 275 to 475 nm, and the strongest peak appears when they are excited at 350 nm.

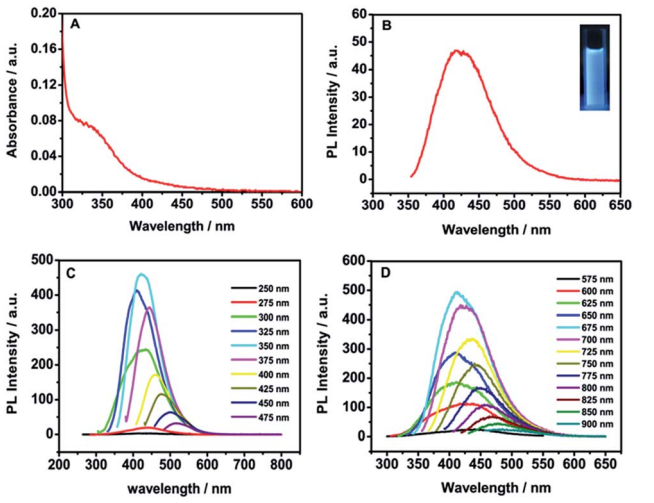


Fig. 4 UV (A) and PL (B) of N,S-GQDs, PL of N,S-GQDs excited with different wavelengths (C and D).

These excitation-dependent fluorescent behaviors were extensively reported in fluorescent carbon-based nanomaterials, and may result from optical transitions of N,S-GQDs with different sizes and surface defects.[32–34] Upconversion fluorescent properties of N,S-GQDs have been observed at excitation wavelengths from 575 to 900 nm. Most interestingly, the upconversion fluorescence also shows an excitation-dependent fluorescent behavior, which is similar to the fluorescence spectra at the excitation wavelength from 275 to 475 nm. This upconverted fluorescent property of N,S-GQDs should be attributed to multiphoton active processes similar to previously reported carbon dots.[24,34]

N-Doped or S-doped carbon materials have shown superior electrocatalytic activity for ORR.[8,10,19] Besides their unique fluorescent properties, electrocatalytic activity for the ORR of N,S-GQDs is also expected. Due to the difficulty in forming a continuous N,S-GQD film and bridging effectively the N,S-GQDs with GCE, RGO prepared by the reduction of GO with hydrazine hydrate was used as assembly template to support the N,S-GQDs (RGO/N,S-GQDs) to research their electrocatalytic activity for the ORR. As can be seen in Fig. S2,† a positive shift of the oxygen reduction peak was observed for the RGO/N,S-GQDs-modified GCE compared with GCE modified with RGO, which confirms the function of N,S-GQDs to promote the ORR of RGO. To investigate the electrocatalytic activities of N,S-RGO/GQDs hybrids, CVs in $O_2$ or $N_2$-saturated 0.1 M KOH solution for GCE modified with N,S-RGO/GQDs hybrids or commercial Pt/C catalyst were measured at a constant mass loading. As shown in Fig. 5B, there is a clear well-defined cathodic peak in the $O_2$-saturated but not the $N_2$-saturated KOH solution for GCE modified with N,S-RGO/GQDs hybrids, which is similar to the commercial Pt/C catalyst (Fig. 5A). The ORR onset potential of

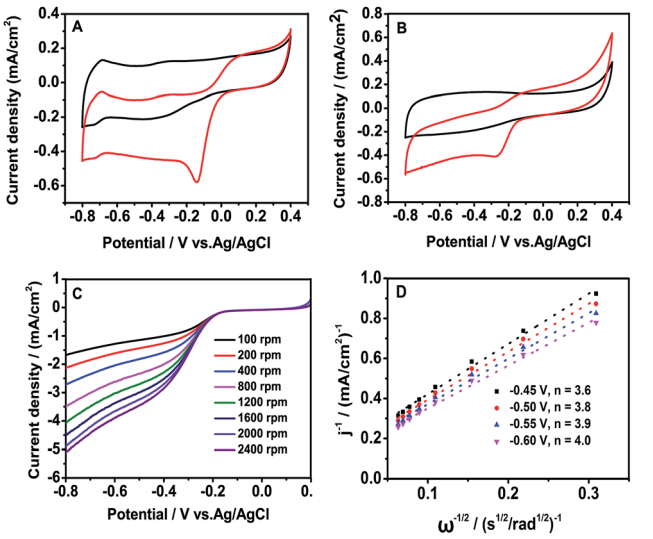


Fig. 5 CVs of (A) commercial Pt/C catalyst and (B) N,S-RGO/GQDs hybrids modified GCE in $N_2$-saturated 0.1 M KOH solution (black), $O_2$-saturated 0.1 M KOH solution (red). Rotating disk electrode (RDE) curves for N,S-RGO/GQDs hybrids in $O_2$-saturated 0.1 M KOH solution with different speeds (C). Koutecky–Levich plots derived from the RDE measurements (D). Scan rate is 5 mV $s^{-1}$.

the commercial Pt/C catalyst is at 0 V, while that of N,S-RGO/GQDs hybrids is at −0.10 V. The reduction peak of the N,S-RGO/GQDs hybrids modified GCE is at −0.25 V, which is close to that of the commercial Pt/C catalyst (−0.16 V) (Fig. 5A). Moreover, N,S-RGO/GQDs hybrids display more positive onset potential and peak potential of the ORR than the RGO, RGO/N,S-GQDs (Fig. S2†), N-doped carbon materials[8,35–37] or S-doped graphene[10] reported previously. These results indicate that N,S-RGO/GQDs hybrids have good catalytic activity and are promising as metal-free catalyst for the ORR in an alkaline solution.

To investigate the reaction mechanism of the ORR process on the N,S-RGO/GQDs hybrids, LSV measurements on a RDE were recorded at different rotating speeds from 100 to 2400 rpm in an $O_2$-saturated 0.1 M KOH solution. It can be observed that the current density of ORR increases with the increase of rotating speed (Fig. 5C), which may be due to the increased diffusion of dissolved oxygen to the surface of modified GCE.[1,19] Koutecky–Levich plots (Fig. 5D) corresponding to the LSV curves in Fig. 5C suggest a first-order reaction for ORR on GCE modified with N,S-RGO/GQDs hybrids.[4,10,19] The limiting current of N,S-RGO/GQDs hybrids at the potential of −0.8 V can reach 4.53 mA $cm^{-2}$ at a rotary speed of 1600 rpm, which is close to Pt/C (Fig. S3†).[44] The transferred electron number per $O_2$ molecule ($n$) involved in the ORR process is calculated to be 3.6–4.0 at the potential from −0.45 to −0.60 V, indicating a four-electron process for ORR on the GCE modified with N,S-RGO/GQDs hybrids.[4,10,19,45] The excellent catalytic activity of N,S-RGO/GQDs hybrids can be explained by the doping of nitrogen and sulfur atoms, which results in different electronegativity on graphene nanosheets with more charged sites which are favorable for the adsorption and reduction of $O_2$.[4,10,47]

Electrocatalytic stability and resistance to crossover effects of catalysts are important for their practical application in fuel cells. The electrocatalytic stability of N,S-RGO/GQDs hybrids towards ORR was examined through continuous potential cycling between −0.8 V and 0.4 V in $O_2$-saturated 0.1 M KOH solution.[46] It can be observed from Fig. 6 that the peak potential and onset potential of the commercial Pt/C for ORR shift negatively after 1000 continuous cycles of CVs, indicating its evident decrease of catalytic activity. 27% of the original response current at −0.6 V for ORR decreases on the commercial Pt/C modified GCE after cycle durability tests. However, only 10.3% of the original response current decreases after 1000 continuous cycles of CVs on the GCE modified with N,S-RGO/GQDs hybrids, indicating the better catalytic stability of N,S-RGO/GQDs hybrids compared with the commercial Pt/C. TEM and HRTEM images in Fig. S4† show that the particle size and crystal lattice spacing of N,S-GQDs don't change evidently in N,S-RGO/GQDs hybrids after cycle durability tests, in comparison with those of samples before cycle durability tests, which confirms the stability of N,S-RGO/GQDs hybrids as ORR catalysts. The resistance to crossover effects was measured by CVs of GCE modified with N,S-RGO/GQDs hybrids and a commercial Pt/C catalyst in an $O_2$-saturated 0.1 M KOH solution, and an $O_2$-saturated 0.1 M KOH solution containing 3 M $CH_3OH$. As shown in Fig. 7A and B, the cathodic peak of GCE modified with the commercial Pt/C catalyst for ORR disappears in the $O_2$-saturated 0.1 M KOH solution containing 3 M $CH_3OH$ coupled with one pair of characteristic peaks derived from methanol reduction/oxidation. GCE modified with N,S-RGO/GQDs hybrids exhibits a stable ORR without any specific electrochemical catalytic activity towards methanol in the electrolyte containing methanol, suggesting that the N,S-RGO/GQDs hybrids have a remarkable tolerance to possible crossover effects.

In order to illustrate the relationship between the structure and electrochemical catalytic activity of the N,S-RGO/GQDs hybrids, N,S-RGO/GQDs hybrids were annealed at 800 °C for 2 h in an Ar atmosphere to further study their electrochemical catalytic activity. The annealed N,S-RGO/GQDs hybrids display a more negative onset potential and peak potential for the ORR than N,S-RGO/GQDs hybrids (Fig. S5†), which indicates that the catalytic activity of N,S-RGO/GQDs hybrids decreases after being annealed at 800 °C for 2 h in an Ar atmosphere. The $n$ value of the annealed N,S-RGO/GQDs hybrids was measured to be 2.1–2.3 at the potential from −0.45 to −0.60 V (Fig. S6†), suggesting a two-electron process for the ORR on GCE modified with the annealed N,S-RGO/GQDs hybrids.[8,10,44]

The change of structure in the N,S-RGO/GQDs hybrids after being annealed at 800 °C for 2 h in the Ar atmosphere was characterized by XPS, which can be seen in Fig. S7.† Two peaks at 401.6 and 405.0 eV appear. The binding energy at 401.6 eV can be ascribed to graphitic nitrogen, and 405.0 eV

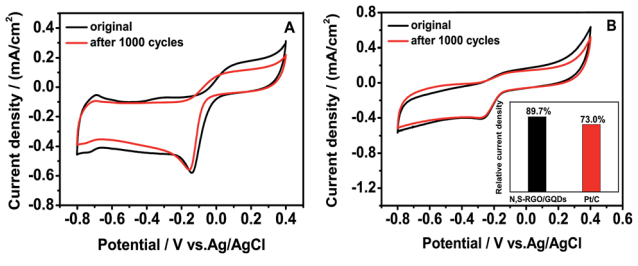


Fig. 6 Electrochemical stability of the commercial Pt/C catalyst (A) and N,S-GQD/RGO hybrids (B) as determined by continuous CVs in $O_2$-saturated 0.1 M KOH solution. Inset is the relative current density of Pt/C and N,S-RGO/GQDs hybrids at −0.6 V after 1000 cycles of CVs. Scan rate is 5 mV $s^{-1}$.

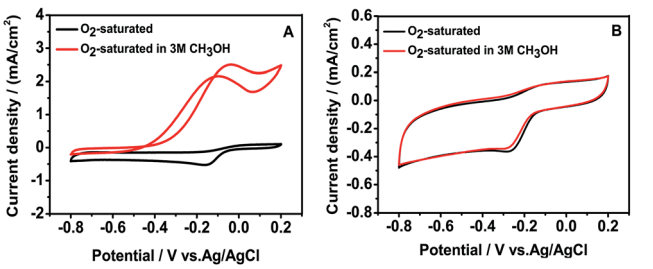


Fig. 7 CVs of commercial Pt/C catalyst (A) and N,S-RGO/GQDs hybrids (B) on GCE in $O_2$-saturated 0.1 M KOH solution, and $O_2$-saturated 0.1 M KOH solution containing 3 M $CH_3OH$. Scan rate is 5 mV $s^{-1}$.

is ascribed to chemisorbed nitrogen oxide.[38,39] The binding energy at 398.4 eV ascribed to the pyridinic nitrogen of the N,S-RGO/GQDs hybrids in Fig. 3B disappears after being annealed. The contrast of XPS characterization between N,S-RGO/GQDs hybrids and the annealed N,S-RGO/GQDs hybrids indicates that the structure of pyridinic nitrogen decreases, and chemisorbed nitrogen oxide forms in the process of being annealed at 800 °C. Furthermore, the sulfur content of N,S-RGO/GQDs hybrids decreased from 1.28 atom% to 0.24 atom% after annealing. The effect of sulfur on the enhanced ORR catalytic activity was proved by previous reports.[10,40] Therefore, it is suggested that the pyridinic nitrogen and sulfur content in the N,S-RGO/GQDs hybrids benefits the highly efficient electrocatalytic activity of N,S-RGO/GQDs hybrids *via* a four-electron pathway for ORR in an alkaline solution.

## Conclusions

In summary, a microwave-assisted and solvothermal method has been developed to prepare excitation-dependent fluorescent N,S-GQDs, and N,S-RGO/GQDs hybrids as a kind of metal-free catalyst for ORR. The prepared N,S-RGO/GQDs hybrids show significantly improved electrocatalytic performance and much better long-term stability than the commercial Pt/C catalysts, which are promising to be applied in fuel cells as a kind of metal-free catalyst for ORR.

## Acknowledgements

This work was financially supported by the National Basic Research Program of China (2012CB933301), the National Natural Science Foundation of China (81273409), the Ministry of Education of China (IRT1148, 20123223110007), the Priority Academic Program Development of Jiangsu Higher Education Institutions (PAPD) and the Postdoctoral Science Foundation of China (2013M541700). Yu Ting thanks the support of the Singapore National Research Foundation under NRF RF award no. NRFRF2010-07.

## Notes and references

1 K. Gong, F. Du, Z. Xia, M. Durstock and L. Dai, *Science*, 2009, **323**, 760–764.
2 M. Lefèvre, E. Proietti, F. Jaouen and J. P. Dodelet, *Science*, 2009, **324**, 71–74.
3 W. Yang, T. P. Fellinger and M. Antonietti, *J. Am. Chem. Soc.*, 2011, **133**, 206–209.
4 J. Liang, Y. Jiao, M. Jaroniec and S. Z. Qiao, *Angew. Chem., Int. Ed.*, 2012, **51**, 11496–11500.
5 B. C. H. Steele and A. Heinzel, *Nature*, 2001, **414**, 345–352.
6 Y. Li, W. Zhou, H. Wang, L. Xie, Y. Liang, F. Wei, J. C. Idrobo, S. J. Pennycook and H. Dai, *Nat. Nanotechnol.*, 2012, **7**, 394–400.
7 Y. Liang, Y. Li, H. Wang, J. Zhou, J. Wang, T. Regier and H. Dai, *Nat. Mater.*, 2011, **10**, 780–786.
8 L. Qu, Y. Liu, J. B. Baek and L. Dai, *ACS Nano*, 2010, **4**, 1321–1326.
9 H. Liu, Y. Liu and D. Zhu, *J. Mater. Chem.*, 2011, **21**, 3335–3345.
10 Z. Yang, Z. Yao, G. Li, G. Fang, H. Nie, Z. Liu, X. Zhou, X. Chen and S. Huang, *Nano*, 2011, **6**, 205–211.
11 Y. Tang, B. L. Allen, D. R. Kauffman and A. Star, *J. Am. Chem. Soc.*, 2009, **131**, 13200–13201.
12 Z. Wang, R. Jia, J. Zheng, J. Zhao, L. Li, J. Song and Z. Zhu, *ACS Nano*, 2011, **5**, 1677–1684.
13 D. Deng, X. Pan, L. Yu, Y. Cui, Y. Jiang, J. Qi, W. X. Li, Q. Fu, X. Ma and Q. Xue, *Chem. Mater.*, 2011, **23**, 1188–1193.
14 R. I. Jafri, N. Rajalakshmi and S. Ramaprabhu, *J. Mater. Chem.*, 2010, **20**, 7114–7117.
15 Y. Li, W. Zhou, H. Wang, L. Xie, Y. Liang, F. Wei, J. C. Idrobo, S. J. Pennycook and H. Dai, *Nat. Nanotechnol.*, 2012, **7**, 394–400.
16 D. Geng, Y. Chen, Y. Li, R. Li, X. Sun, S. Ye and S. Knights, *Energy Environ. Sci.*, 2011, **4**, 760–764.
17 F. Jaouen, J. Herranz, M. Lefèvre, J. P. Dodelet, U. I. Kramm, I. Herrmann, P. Bogdanoff, J. Maruyama, T. Nagaoka, A. Garsuch, *et al.*, *ACS Appl. Mater. Interfaces*, 2009, **1**, 1623–1639.
18 Y. Zhang, K. Fugane, T. Mori, L. Niu and J. Ye, *J. Mater. Chem.*, 2012, **22**, 6575–6580.
19 Y. Li, Y. Zhao, H. Cheng, Y. Hu, G. Shi, L. Dai and L. Qu, *J. Am. Chem. Soc.*, 2012, **134**, 15–18.
20 D. Pan, J. Zhang, Z. Li and M. Wu, *Adv. Mater.*, 2010, **22**, 734–738.
21 X. Yan, X. Cui, B. Li and L. Li, *Nano Lett.*, 2010, **10**, 1869–1873.
22 X. Yan, X. Cui and L. Li, *J. Am. Chem. Soc.*, 2010, **132**, 5944–5945.
23 Y. Li, Y. Hu, Y. Zhao, G. Shi, L. Deng, Y. Hou and L. Qu, *Adv. Mater.*, 2011, **23**, 776–780.
24 J. Shen, Y. Zhu, C. Chen, X. Yang and C. Li, *Chem. Commun.*, 2011, **47**, 2580–2582.
25 W. S. Hummers Jr and R. E. Offeman, *J. Am. Chem. Soc.*, 1958, **80**, 1339.
26 I. Vlasov, O. I. Lebedev, V. G. Ralchenko, E. Goovaerts, G. Bertoni, G. Van Tendeloo and V. I. Konov, *Adv. Mater.*, 2007, **19**, 4058–4062.
27 J. Zang, Y. Wang, L. Bian, J. Zhang, F. Meng, Y. Zhao, R. Lu, X. Qu and S. Ren, *Carbon*, 2012, **50**, 3032–3038.
28 J. Zhou, C. Booker, R. Li, X. Zhou, T. K. Sham, X. Sun and Z. Ding, *J. Am. Chem. Soc.*, 2007, **129**, 744–745.
29 Z. H. Sheng, L. Shao, J. J. Chen, W. J. Bao, F. B. Wang and X. H. Xia, *ACS Nano*, 2011, **5**, 4350–4358.
30 Y. Shao, S. Zhang, M. H. Engelhard, G. Li, G. Shao, Y. Wang, J. Liu, I. A. Aksay and Y. Lin, *J. Mater. Chem.*, 2010, **20**, 7491–7496.
31 S. Cho, J. H. Seo, S. H. Park, S. Beaupré, M. Leclerc and A. J. Heeger, *Adv. Mater.*, 2010, **22**, 1253–1257.
32 D. Pan, J. Zhang, Z. Li and M. Wu, *Adv. Mater.*, 2010, **22**, 734–738.
33 S. Zhuo, M. Shao and S. T. Lee, *ACS Nano*, 2012, **6**, 1059–1064.

 

34 S. Zhu, J. Zhang, C. Qiao, S. Tang, Y. Li, W. Yuan, B. Li, L. Tian, F. Liu, R. Hu, H. Gao, H. Wei, H. Zhang, H. Sun and B. Yang, *Chem. Commun.*, 2011, **47**, 6858–6860.
35 R. Liu, D. Wu, X. Feng and K. Müllen, *Angew. Chem.*, 2010, **122**, 2619–2623.
36 Z. Luo, S. Lim, Z. Tian, J. Shang, L. Lai, B. MacDonald, C. Fu, Z. Shen, T. Yu and J. Lin, *J. Mater. Chem.*, 2011, **21**, 8038–8044.
37 Y. Ma, L. Sun, W. Huang, L. Zhang, J. Zhao and Q. Fan, *J. Phys. Chem. C*, 2011, **115**, 24592–24597.
38 R. Arrigo, M. Havecker, R. Schlogl and D. S. Su, *Chem. Commun.*, 2008, 4891–4893.
39 H. Liu, Y. Zhang, R. Li, X. Sun, S. Désilets, H. Abou-Rachid, M. Jaidann and L. S. Lussier, *Carbon*, 2010, **48**, 1498–1507.
40 H. Chung, C. Johnston, K. Artyushkova, M. Ferrandon, D. Myers and P. Zelenay, *Electrochem. Commun.*, 2010, **12**, 1792–1795.
41 Z. Luo, L. Yuwen, B. Bao, J. Tian, X. Zhu, L. Weng and L. Wang, *J. Mater. Chem.*, 2012, **22**, 7791–7796.
42 Z. Luo, L. Yuwen, Y. Han, J. Tian, X. Zhu, L. Weng and L. Wang, *Biosens. Bioelectron.*, 2012, **36**, 179–185.
43 Z. Luo, X. Ma, Y. Han, L. Yuwen, X. Zhu, L. Weng and L. Wang, *Carbon*, 2013, **57**, 470–476.
44 D. Geng, Y. Chen, Y. Chen, Y. Li, R. Li, X. Sun, S. Ye and S. Knights, *Energy Environ. Sci.*, 2011, **4**, 760–764.
45 Y. Liu and P. Wu, *ACS Appl. Mater. Interfaces*, 2013, **5**, 3362–3369.
46 K. Huang, K. Sasaki, R. R. Adzicb and Y. Xing, *J. Mater. Chem.*, 2012, **22**, 16824–16832.
47 W. Ai, Z. Luo, J. Jiang, J. Zhu, Z. Du, Z. Fan, L. Xie, H. Zhang, W. Huang and T. Yu, *Adv. Mater.*, 2014, **26**, 6186–6192.